

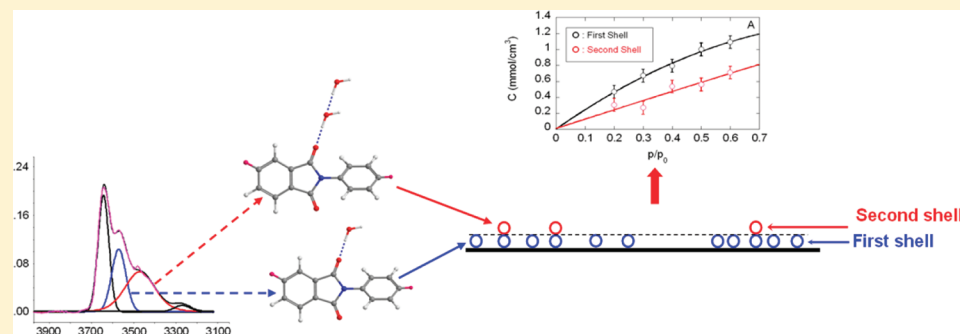
# Combining Gravimetric and Vibrational Spectroscopy Measurements to Quantify First- and Second-Shell Hydration Layers in Polyimides with Different Molecular Architectures

Pellegrino Musto,<sup>\*,†</sup> Giuseppe Mensitieri,<sup>‡</sup> Marino Lavorgna,<sup>§</sup> Gennaro Scarinzi,<sup>†</sup> and Giuseppe Scherillo<sup>‡</sup>

<sup>†</sup>Institute of Chemistry and Technology of Polymers, National Research Council of Italy, Via Campi Flegrei 34, Olivetti Buildings, 80078, Pozzuoli (NA), Italy

<sup>‡</sup>Department of Materials and Production Engineering, University of Naples "Federico II", Piazzale Tecchio 80, 80125 Naples, Italy

<sup>§</sup>Institute of Composite and Biomedical Materials, National Research Council of Italy, Piazzale Tecchio, 80-80125 Naples, Italy



**ABSTRACT:** In-situ Fourier transform infrared (FTIR) measurements have been carried out at different relative pressures of water vapor to study the  $\text{H}_2\text{O}$  diffusion in three polyimides differing in their molecular structure and fluorine substitution. Spectral data have been analyzed by difference spectroscopy, least-squares curve fitting, and two-dimensional (2D) correlation spectroscopy, which provided molecular level information on the diffusion mechanism. In particular, two distinct water species were identified corresponding, respectively, to the first and second-shell hydration layers. The spectroscopic analysis demonstrated that the relative population of these species is a function of the total water content in the system. A method has been devised to quantify the water concentration in the two hydration layers, based on a combination of spectroscopic and gravimetric data. The results have been compared with those from an earlier spectroscopic approach reported in the literature and based on the analysis of the carbonyl region.

## 1. INTRODUCTION

Polyimides are a family of heterocyclic polymers possessing a favorable combination of price, processability, and performance that makes them attractive for many advanced applications. The elevated thermo-oxidative and chemical stability, coupled with good mechanical properties, makes these polymers the ideal candidates for use in harsh environments.<sup>1–3</sup> A further important field where certain polyimides find application is that of separation membranes.<sup>4</sup> There has been considerable activity in the study of novel polyimides structurally modified to enhance gas flow through their films.<sup>5</sup> It became apparent that in these novel structures the flow increase was not uniform for all gases, thus making feasible gas separation and enrichment processes. The aforementioned studies were prompted by the versatility of the polyimide synthesis, which renders the preparation of sophisticated molecular structures a relatively straightforward task.<sup>3,5</sup>

In order to take full advantage of the peculiar sorption properties of polyimides, it is necessary to gain a deep understanding of the mass-transport mechanism and how it is influenced by the chain structure of the membrane. This is particularly true for those penetrants that are able to establish molecular interaction

with the polymer, as is the case of water. Water diffusion in polyimides is a complex process that has received considerable attention in recent years owing to its technological relevance.<sup>6–8</sup> Previous contributions have highlighted the importance of the "interaction effect" and of the molecular structure of the polymer substrate in controlling the diffusion behavior.<sup>9,10</sup> Toward a complete description of the mass-transport mechanism, which is a prerequisite to any attempt at developing a predictive modeling scheme, the issues to be addressed are manifold: (i) the type of molecular interactions, (ii) the interaction site(s) on the polymer backbone, (iii) the nature and the number of the penetrant species, and, above all, (iv) a method to quantitatively estimate the population of the different species present in the system both at equilibrium and during their dynamic evolution.

The most sensitive experimental technique to investigate H-bonding systems is infrared spectroscopy, which has been extensively used to characterize  $\text{H}_2\text{O}$  molecules absorbed in

Received: June 17, 2011

Revised: December 27, 2011

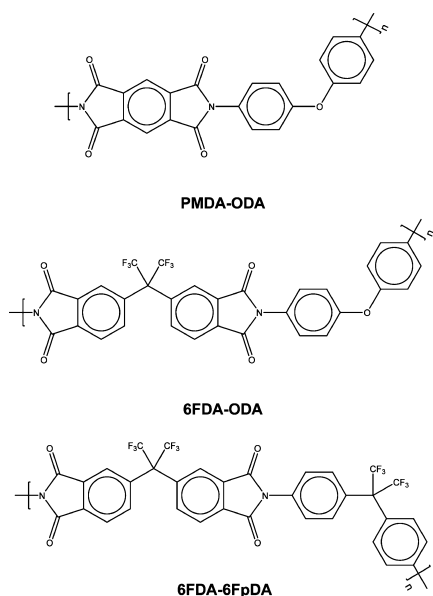
Published: December 28, 2011

macromolecular media.<sup>11–15</sup> Problems arise, however, to fully exploit the wealth of molecular information contained in the vibrational spectrum, owing to the intrinsic breath of the  $\nu(\text{OH})$  band and the enhancement of its molar absorptivity upon the establishment of the interaction. The latter effect is poorly predictable on a theoretical ground and is hardly amenable to direct measurement, which makes the quantitative analysis a rather difficult task. Several approaches have been proposed in the literature to solve these problems, notably those of Marechal,<sup>11–13</sup> recently summarized in a comprehensive review.<sup>11</sup> In the present contribution *time-resolved* Fourier transform infrared (FTIR) measurements have been performed at different relative pressures of water vapor to investigate the  $\text{H}_2\text{O}$  diffusion in three polyimides differing for their molecular structure and fluorine substitution. The spectral data have been analyzed by different and complementary approaches, i.e., difference spectroscopy, least-squares curve fitting (LSCF) and two-dimensional correlation spectroscopy (2D-COS), which provided information on the nature and the number of water species present in the systems. A method has been proposed to quantify the population of the above species, based on the evaluation of the respective molar absorptivities. These were obtained by coupling the spectroscopic data with gravimetric measurements carried out in the same conditions. The data obtained in the present work will form the basis for developing a predictive model, to be discussed in a forthcoming contribution, aimed at simulating the thermodynamics of water sorption in polyimides and accounting for self- and cross-hydrogen bonding interactions.

## 2. EXPERIMENTAL SECTION

**Materials.** The molecular structures of the three investigated polyimides are reported in Scheme 1. The PMDA-ODA

Scheme 1



was obtained by thermal imidization of its polyamic acid precursor, Pyre-ML RK692 from IST (Indian Orchard, MA). This precursor had molecular weights  $M_w = 1.0 \times 10^5$  g/mol and  $M_n = 4.6 \times 10^4$  g/mol and was supplied as a 12 wt % solution in a *N*-methyl-2-pyrrolidone (NMP)/xylene mixture (80/20 wt/wt). The 6FDA-ODA and 6FDA-6FpDA polyamic

acid precursors were synthesized from the respective dianhydride and diamine monomers [(hexahydrofluoroisopropylidene) diphthalic anhydride (6FDA), 4,4'-diaminodiphenyl ether (ODA), 4,4'-(hexafluoroisopropylidene) dianiline (6FpDA)], according to the procedures described in ref 16. The monomers, purchased from Sigma-Aldrich (St. Louis, MO), were purified by vacuum sublimation and stored under vacuum. NMP, also from Sigma-Aldrich, was stirred overnight over phosphorus pentoxide and stored under nitrogen. In Table 1 are summarized some characterization data relative to the three polyimides.

Table 1. Properties of the Investigated Polyimides

polyimide	$\eta_{\text{red}}^a$ (dL/g)	$T_g^{\text{DSC}}{}^b$ (°C)	$T_g^{\text{DMTA}}{}^c$ (°C)	density <sup>d</sup> (g/cm <sup>3</sup> )
PMDA-ODA			383	1.405
6FDA-ODA	1.60	302	308	1.510
6FDA-6FpDA	0.72	312	315	1.610

<sup>a</sup>Reduced viscosity; concentration: 0.50 g/dL in NMP at 30 °C.

<sup>b</sup>Differential scanning calorimetry; heating rate: 20 °C/min. <sup>c</sup>Dynamical-mechanical thermal analysis; heating rate: 5 °C/min; frequency = 1 Hz. <sup>d</sup>Density by helium picnometry.

**Preparation of the Polyimide Films.** Castings 20–30 μm thick were obtained by spreading the polyamic acid solution onto a glass support with the use of a calibrated Gardner knife, which allows one to control the film thickness in the range 10–40 μm. The cast films were dried 1 h at room temperature and 1 h at 80 °C to allow most of the solvent to evaporate. Afterward, the castings were cured stepwise at 100, 150, 200, 250, and 290 °C for 1 h at each temperature. The cured films were removed from the glass substrate by immersion in distilled water at 80 °C.

Thinner films (3.0–1.0 μm) were prepared by a two-step, spin-coating process performed with a Chemat KW-4A apparatus equipped with an automated fluid dispenser (KW-4AD) from Chemat Technologies Inc. (Northridge, CA). Spinning conditions were 12 s at 700 rpm for the first step and 20 s at 1500 rpm for the second step. Fifteen weight percent solutions of the polyamic acid precursors in NMP were used to feed the fluid dispenser. The spin-coated substrates were cured in the same conditions as for the thicker films, and free-standing samples were removed in distilled water at room temperature.

**FTIR Spectroscopy.** A vacuum-tight FTIR cell purposely designed and built, was used to perform the time-resolved acquisition of FTIR spectra during the sorption experiments. Data collection on the polymer films exposed to water vapor at constant relative pressures was carried out in the transmission mode. The cell, positioned in the sample compartment of the spectrometer, was connected through service-lines, to a water reservoir, a turbo-molecular vacuum pump, and pressure transducers. Full details of the experimental setup are reported in refs 14 and 17.

The FTIR spectrometer was a Spectrum GX from Perkin-Elmer (Norwalk, CT), equipped with a Ge/KBr beam splitter and a wide-band DTGS detector. The instrumental parameters for data collection were as follows: resolution = 4 cm<sup>-1</sup>; optical path difference (OPD) velocity = 0.5 cm/s, spectral range 4000–400 cm<sup>-1</sup>. A single data collection per spectrum was performed, which took 2.0 s to complete in the selected instrumental conditions. Spectra were acquired in the single-beam mode for subsequent data processing. Automated data acquisition was

controlled by a dedicated software package for time-resolved spectroscopy (timebase from Perkin-Elmer).

Sorption tests were performed at 30 °C and at relative pressures of water vapor,  $p/p_0$ , ranging from 0.1 to 0.6 for the spectroscopic measurements, and from 0.1 to 0.8 for the gravimetric measurements.

**FTIR Data Analysis.** Full absorbance spectra (i.e., polyimide plus sorbed water) were obtained using as background the cell without sample at the test conditions. The spectra representative of sorbed water were obtained by using as background the single-beam spectrum of the cell containing the dry polyimide film. This allows one to eliminate the interference of the polyimide spectrum in the regions of interest. It is explicitly noted that this data processing approach is equivalent to the more general difference spectroscopy method provided that no changes in sample thickness take place during the measurement.<sup>9</sup> This has been verified in the present case. Difference spectroscopy has also been used to analyze the carbonyl band shape, in which case the subtraction factor,  $K$ , holds quantitative information on concentration ratios.<sup>9</sup>

Curve fitting analysis was performed by a Levenberg–Marquardt least-squares algorithm.<sup>18,19</sup> The peak function used throughout was a mixed Gauss–Lorentz line shape of the form<sup>19</sup>

$$f(x) = (1 - Lr)H \exp - \left[ \left( \frac{x - x_0}{w} \right)^2 (4 \ln 2) \right] + Lr \frac{H}{4 \left( \frac{x - x_0}{w} \right)^2 + 1} \quad (1)$$

where  $x_0$  is the peak position;  $H$  is the peak height;  $w$  is the full-width at half height (fwhh) and  $Lr$  is the fraction of Lorentz character. In order to keep the number of adjustable parameters to a minimum, the baseline and the number of components were fixed, allowing the curve-fitting algorithm to optimize the fwhh, the position of the individual component, and the band-shape (Lr parameter).

2D-COS analysis was performed on an evenly spaced sequence of 20 spectra collected with a sampling interval of 12 s. For the notation adopted to identify the peaks in the correlation spectra, refer to ref 9.

**Gravimetric Measurements.** The equipment used to determine the weight gain of samples exposed to a controlled humidity environment is analogous to that used for the spectroscopic measurements, with an electronic microbalance D200 from Cahn Instruments (Madison, WI), in place of the FTIR diffusion chamber. The microbalance provides a sensitivity of 0.1 µg with an accuracy of  $\pm 0.2$  µg.

### 3. RESULTS AND DISCUSSION

**Comparative Analysis of Absorbance and Difference Spectra.** Sorption of water in polyimides results in the appearance of well-defined bands characteristic of the multiplicity of penetrant species present in the system. In Figures 1–3 are compared the spectra of the dry polyimides with those of the samples after equilibration with water vapor at a relative pressure of 0.6. The prominent water bands, highlighted in the figures, are observed in the 3800–3200 cm<sup>-1</sup> region ( $\nu_{\text{OH}}$ ) and 1680–1570 cm<sup>-1</sup> region ( $\delta_{\text{HOH}}$ ).

The suppression of the polymer matrix interference by use of difference spectroscopy,<sup>9,17</sup> allows one to isolate the spectrum of absorbed water in the different environments.

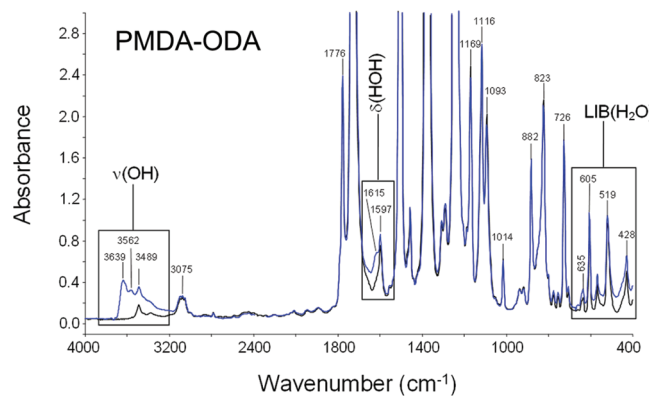


**Figure 1.** FTIR spectra in the 4000–400 cm<sup>-1</sup> range for the PMDA-ODA polyimide in the dry state (black trace) and after equilibration at  $p/p_0 = 0.6$  (blue trace). Sample thickness  $20 \pm 0.5 \mu\text{m}$ .

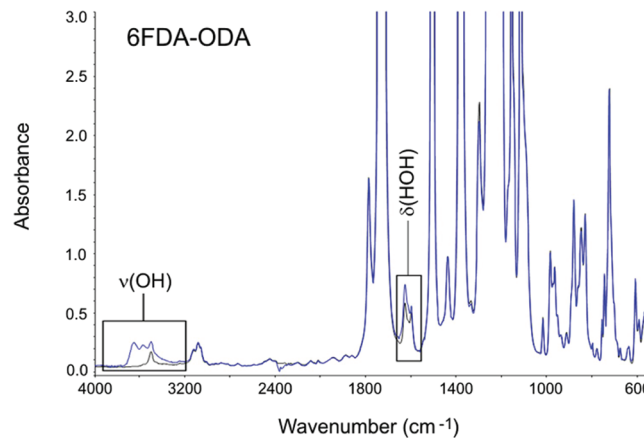


**Figure 2.** FTIR spectra in the 4000–550 cm<sup>-1</sup> range for the 6FDA-ODA polyimide in the dry state (black trace) and after equilibration at  $p/p_0 = 0.6$  (blue trace). Sample thickness  $27 \pm 0.5 \mu\text{m}$ .

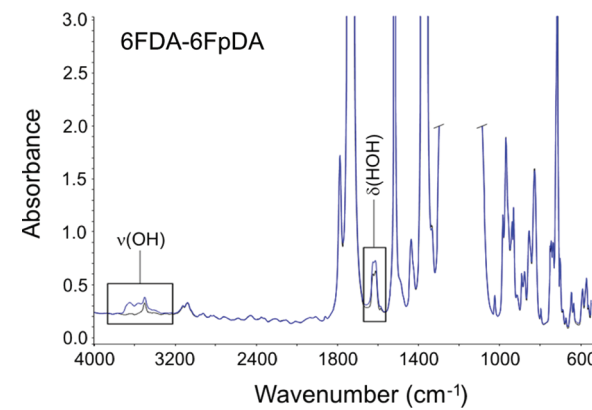


**Figure 3.** FTIR spectra in the 4000–550 cm<sup>-1</sup> range for the 6FDA-6FpDA polyimide in the dry state (black trace) and after equilibration at  $p/p_0 = 0.6$  (blue trace). Sample thickness  $36 \pm 0.5 \mu\text{m}$ .

These spectra are compared in Figure 4A,B for the bending and the stretching regions, respectively. The spectra evidence significant differences in terms of total sorbed water among the three investigated polyimides. As expected, the amount of sorbed water decreases considerably with increasing the fluorine content.

The band-shape of the bending mode is essentially coincident in all cases and does not show evidence of a multi-component structure. The lack of resolution in this frequency

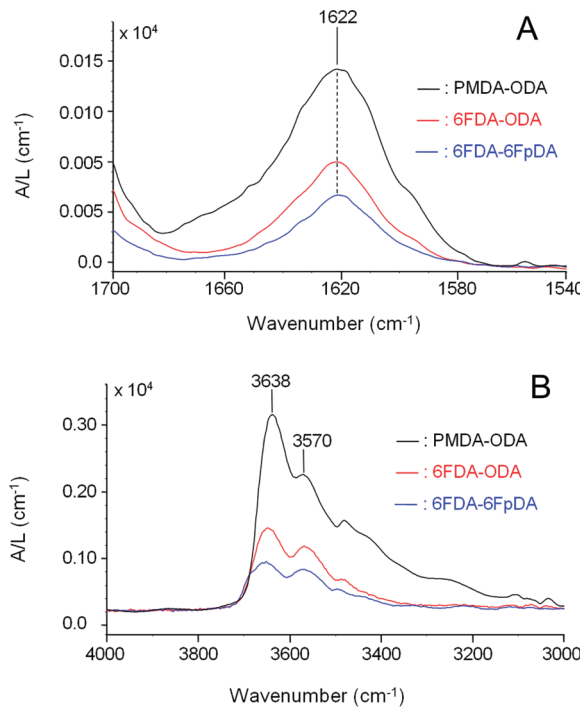


**Figure 4.** Difference spectra (wet–dry) normalized for the sample thickness, representative of water absorbed in the three investigated polyimides. (A) 1700–1540  $\text{cm}^{-1}$  wavenumber range; (B) 4000–3000  $\text{cm}^{-1}$  wavenumber range. Spectra denoted as wet were collected at equilibrium at  $p/p_0 = 0.6$ .

range is to be expected in view of the low sensitivity of the  $\delta(\text{HOH})$  vibration toward H-bonding.

Conversely, the  $\nu_{\text{OH}}$  profile displays a complex, well-resolved band-shape, which indicates the occurrence of distinct water species involved in H-bonding interactions. In the three polyimides the spectra appear to be quite similar, but in fact, subtle differences exist, as will be discussed in detail in the forthcoming paragraphs.

Time-resolved data collected *in situ* during sorption/desorption tests can be used to precisely monitor the diffusion kinetics.<sup>9,11–13,17</sup> This is demonstrated in Figure 5, where the

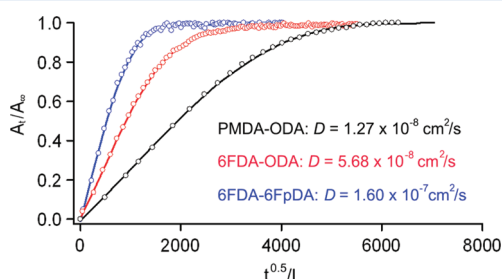


**Figure 5.** Fick's diagrams for the three investigated polyimides. Sorption tests carried out at  $p/p_0 = 0.4$ .

relative absorbance of the 1620  $\text{cm}^{-1}$  water band is reported in a Fick's diagram, i.e., as a function of  $\sqrt{t}/L$ , where  $t$  is the time and  $L$  is the sample thickness. As generally observed for polyimides, the diffusion behavior is typically Fickean, but the diffusivity values change markedly among the three polymers investigated herein. In particular, the fully fluorinated polyimide exhibits a  $D$  value more than 1 order of magnitude higher than

that of the nonfluorinated polyimide, while the 6FDA-ODA displays an intermediate value.

Sorption isotherms in the range of relative pressures from 0.1 to 0.6 have been measured both spectroscopically and gravimetrically. The gravimetric data, reported in Figure 6,

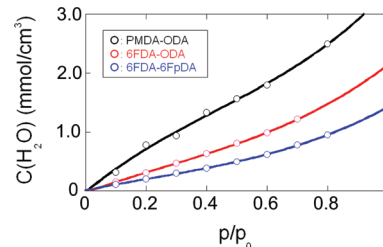


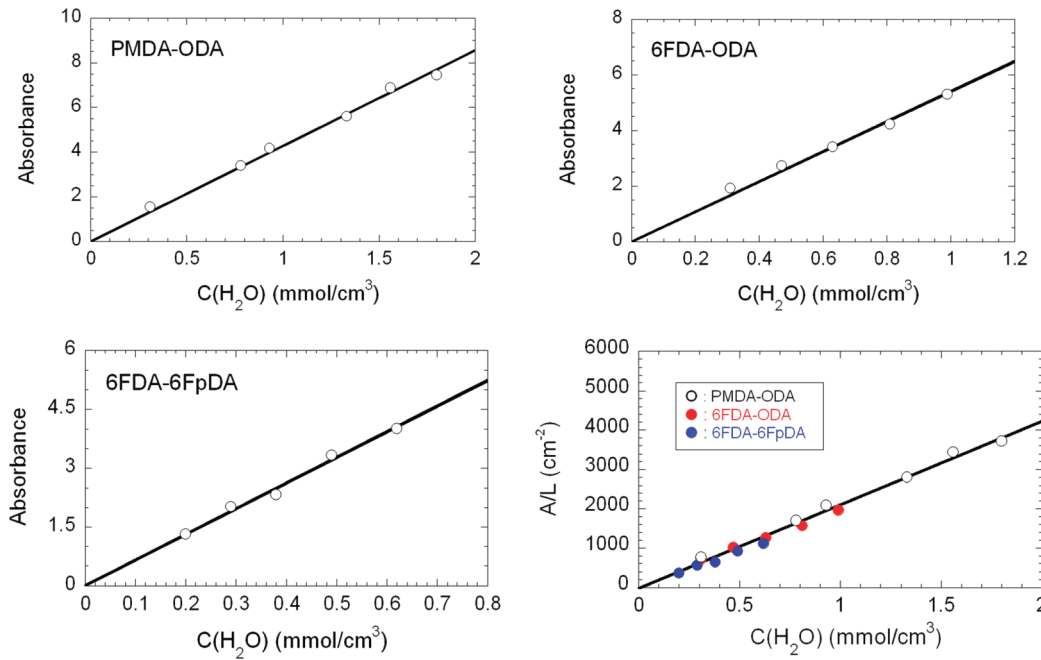
**Figure 6.** Water vapor sorption isotherms as measured gravimetrically for the three investigated polyimides.

demonstrate that the nonfluorinated polyimide exhibits the higher sorption capacity, which, at  $p/p_0 = 0.6$ , exceeds those of 6FDA-ODA and 6FDA-6FpDA by a factor of about 2 and 3, respectively.

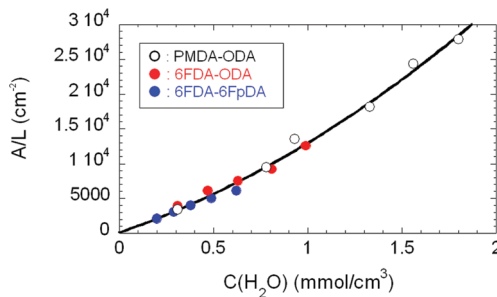
The upturn present in sorption isotherms is generally attributed to two different factors: (1) plasticization of the glassy matrix induced by the penetrant, which promotes the transition from a glassy to a rubbery system,<sup>20</sup> and (2) the gradual onset of penetrant clustering or self-association as the relative pressure increases.<sup>21</sup> In view of the high glass transition temperature of the three investigated polyimides (exceeding 300 °C) and of the relatively low amount of sorbed water, the second interpretation is to be considered as the most likely.

Figure 7 reports the correlations between the intensity of the  $\delta(\text{HOH})$  peak and the water concentration evaluated gravimetrically. In particular, the first three plots represent the integrated area of the 1622  $\text{cm}^{-1}$  band for the individual polyimides, while the fourth diagram collects together the three data sets into a single master curve after absorbance normalization for sample thickness. A highly linear correlation through the origin (average correlation coefficient = 0.998) is apparent in all cases, according to the Beer–Lambert relationship.<sup>22</sup> When the same diagram is constructed by considering the absorbance area of the  $\nu(\text{OH})$  band (see Figure 8), the data can be still accommodated on a single master curve, but now a significant departure from linearity is observed for concentration values exceeding 0.75  $\text{mmol}/\text{cm}^3$ . The very high correlation degree between the spectroscopic and gravimetric data relative to the three polyimides for both the stretching and the bending frequency ranges, points to the conclusion that, for all the considered vibrational modes, the absorptivity values of the different water species are independent of the particular polyimide system. The upturn observed in Figure 8 at higher values of water concentration qualitatively indicates an increase in the relative concentration of water species characterized by higher absorptivity values (more on this later). As detailed in the forthcoming paragraphs, the correlations between the gravimetric and the spectroscopic data will form the basis for a method to quantify the population of the different water species present in the investigated systems.

**2D-COS.** To investigate in detail the behavior of polymer-penetrant systems from an interactional standpoint, 2D-FTIR correlation spectroscopy (2D-COS) has emerged as one of the most effective tools.<sup>9,23,24</sup> This technique is capable of improving the resolution by spreading the data over a second frequency axis



**Figure 7.** Absorbance of the  $\delta(\text{HOH})$  band as a function of water concentration as evaluated gravimetrically for the three investigated polyimides. The fourth diagram reports all the data points after absorbance normalization for sample thickness.



**Figure 8.** Absorbance of the  $\nu(\text{OH})$  band normalized for sample thickness as a function of water concentration as evaluated gravimetrically for the three investigated polyimides.

and, at the same time, can provide information about the dynamics of the evolving system. The asynchronous correlation maps obtained from the time-resolved FTIR spectra collected in situ during water vapor sorption tests at  $p/p_0 = 0.6$  are reported in Figure 9, and the analysis results are collected in Table 2A–C.

We recall that a peak in the asynchronous spectrum at  $[\nu_1, \nu_2]$  corresponds to two IR signals changing at different rates. On the other hand, a zero intensity is obtained when two signals change at the same rate, thus providing the characteristic resolution enhancement and the specificity of the asynchronous pattern. Moreover, the sign of the asynchronous peaks supplies information about the sequence of changes of the two correlated IR signals, according to the so-called Noda rules.<sup>23,24</sup>

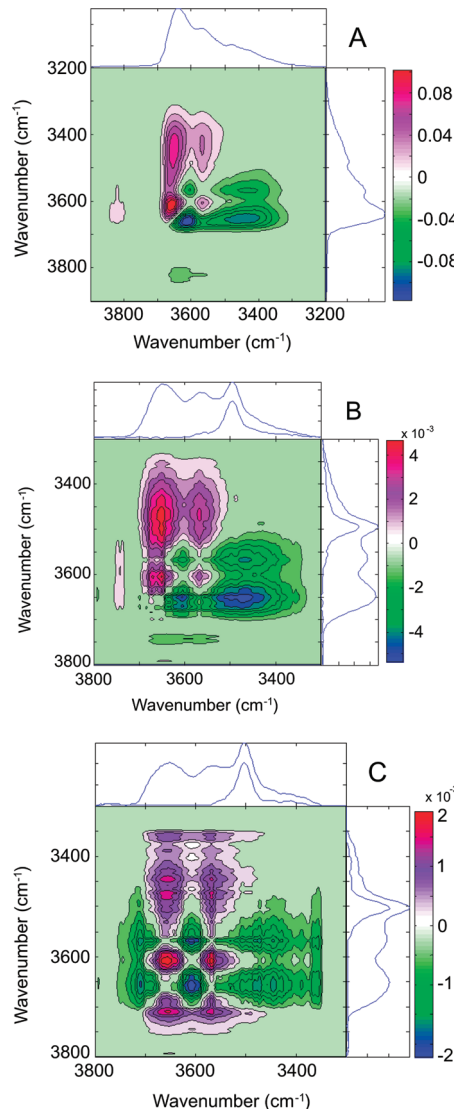
The asynchronous spectrum for the case of water sorption in PMDA-ODA (Figure 9 and Table 2A) displays four cross-peaks, centered, respectively, at  $[3660–3660 \text{ cm}^{-1} (-)]$ ,  $[3570–3616 \text{ cm}^{-1} (+)]$ ,  $[3456–3660 \text{ cm}^{-1} (-)]$ , and  $[3456–3570 \text{ cm}^{-1} (-)]$ . No asynchronous correlation was found at  $3660–3570 \text{ cm}^{-1}$  and at  $3616–3456 \text{ cm}^{-1}$ . The whole of the 2D results suggests the presence of a couple of signals at  $3660–3570 \text{ cm}^{-1}$  and a couple of signals at  $3616–3456 \text{ cm}^{-1}$ ; the two components of each couple change at the same rate, but the two couples

exhibit different dynamics. According to the general observation that a single water molecule produces two OH-stretching modes (in-phase at lower frequency and out-of-phase at higher frequency), the above findings can be interpreted by assuming the occurrence of two distinct water species. In particular, the signs of the correlation peaks indicate that, in the sorption test, the concentration of the species absorbing at  $3660–3570 \text{ cm}^{-1}$  increases faster than the concentration of the species absorbing at  $3616–3456 \text{ cm}^{-1}$ .

A very close pattern is found for the case of 6FDA-ODA (Figure 9B, Table 2B), pointing to the presence of the same interacting species as for PMDA-ODA. The dynamic behavior of the two water species is also coincident with that in PMDA-ODA.

Conversely, in the case of 6FDA-6FpDA, two additional correlation peaks are observed at  $[3660–3700 \text{ cm}^{-1} (+)]$  and  $[3570–3700 \text{ cm}^{-1} (+)]$ . This result indicates the presence of a further component at  $3700 \text{ cm}^{-1}$  which evolves at the same rate as the doublet at  $3616–3456 \text{ cm}^{-1}$  (no correlations observed at the respective frequencies) and at a slower rate compared to the doublet at  $3660–3570 \text{ cm}^{-1}$ . The vibrational assignment of the signals identified so far needs the specification of the molecular environment of the water molecules, i.e., the identification of the active site(s) of the polymer. The discussion is therefore postponed after the analysis of the polyimide spectrum.

**The Polymer Active Site.** The site of interaction on the polymer backbone was identified by investigating the perturbation of the polyimide spectrum induced by the presence of absorbed water. The samples used for diffusion kinetics were unsuitable for this purpose because the use of films  $20–35 \mu\text{m}$  thick makes most of the polyimide signals higher than the saturation threshold (see Figures 1–3). The analysis requires films with a thickness between  $1.0$  and  $3.5 \mu\text{m}$ , which were prepared ad hoc by a spin-coating process (see Experimental Section). Spectroscopic evidence of the involvement of imide carbonyls in H-bonding interactions with sorbed water was then provided by a red shift of both the  $\nu_{\text{as}}(\text{C}=\text{O})$  and the  $\nu_s(\text{C}=\text{O})$  modes observed for the PMDA-ODA and the 6FDA-ODA polyimides (see Figure 10A,B).



**Figure 9.** 2D-FTIR correlation spectra (asynchronous) obtained from the time-resolved spectra collected during the sorption experiment at  $p/p_0 = 0.6$ . Data relative to (A) PMDA-ODA; (B) 6FDA-ODA; (C) 6FDA-6FpDA.

This shift, at sorption equilibrium, is found to increase with increasing water concentration, and is fully reversible upon removal of the sorbed water.<sup>9</sup>

In Figure 11A are compared the IR spectra of the fully dry PMDA-ODA (blue trace) and of the same polyimide film after equilibration at  $p/p_0 = 0.6$  (red trace). The scale-expanded difference spectrum (wet-dry) is also reported. The comparison is made in three distinct frequency ranges of the spectrum where are located intense peaks characteristic of potential proton-acceptor groups. Figure 11B displays the same comparison for dry and wet 6FDA-ODA.

It is noted that, for both polyimides, while the two carbonyl components are shifted toward lower wavenumbers, the  $1378\text{ cm}^{-1}$  band is displaced in the opposite direction. The red shift of the  $\nu(\text{C=O})$  peaks is to be related to the lowering of the force constant of the  $\text{C=O}$  bond caused by the H-bonding. To account for the blue shift of the  $1378\text{ cm}^{-1}$  band, we recall that previous literature reports<sup>25,26</sup> and a recent normal coordinate analysis carried out on the model system *N*-phenylphthalimide- $\text{H}_2\text{O}$ <sup>9</sup> demonstrated that the aforementioned normal mode

**Table 2**

A. Correlation Peaks in the Asynchronous Spectrum as Obtained from a Water Sorption Test on PMDA-ODA at $p/p_0 = 0.6$			
$\nu_1$ ( $\text{cm}^{-1}$ )	$\nu_2$ ( $\text{cm}^{-1}$ )	sign	relative rate of change
3616	3660	—	$3616 < 3660$
3570	3616	+	$3570 > 3616$
3456	3660	—	$3456 < 3660$
3456	3570	—	$3456 < 3570$
B. Correlation Peaks in the Asynchronous Spectrum as Obtained from a Water Sorption Test on 6FDA-ODA at $p/p_0 = 0.6$			
$\nu_1$ ( $\text{cm}^{-1}$ )	$\nu_2$ ( $\text{cm}^{-1}$ )	sign	relative rate of change
3616	3660	—	$3616 < 3660$
3570	3616	+	$3570 > 3616$
3456	3660	—	$3456 < 3660$
3456	3570	—	$3456 < 3570$
C. Correlation Peaks in the Asynchronous Spectrum as Obtained from a Water Sorption Test on 6FDA-6FpDA at $p/p_0 = 0.6$			
$\nu_1$ ( $\text{cm}^{-1}$ )	$\nu_2$ ( $\text{cm}^{-1}$ )	sign	relative rate of change
3660	3700	+	$3660 > 3700$
3616	3660	—	$3616 < 3660$
3570	3700	+	$3570 > 3700$
3570	3616	+	$3570 > 3616$
3456	3660	—	$3456 < 3660$
3456	3570	—	$3456 < 3570$

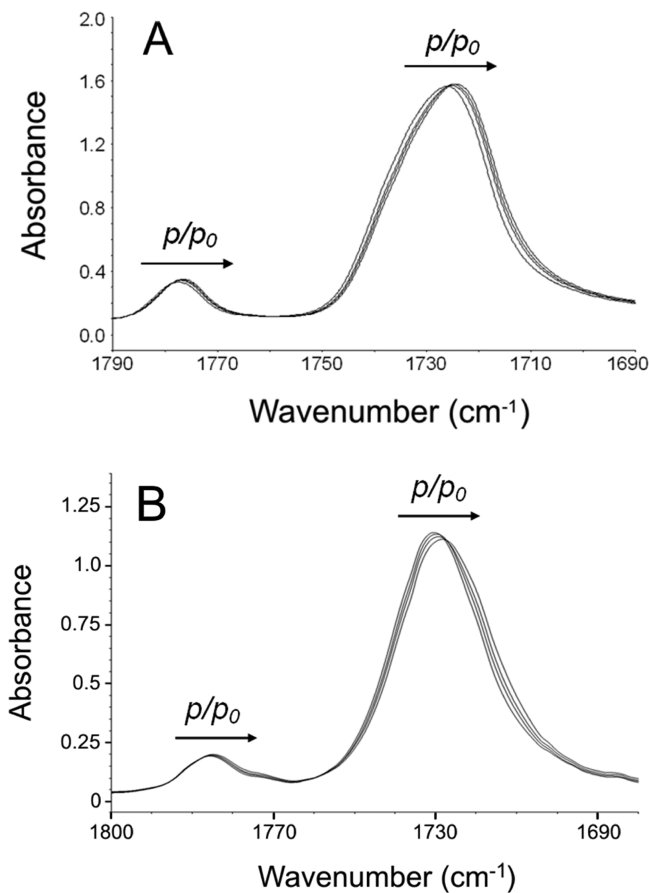


**Figure 10.** The carbonyl stretching region at sorption equilibrium at different  $p/p_0$  values. (A) PMDA-ODA; (B) 6FDA-ODA.

contains a significant contribution from the N-C-O in-plane deformation, whose force constant is known to be stiffened upon the establishment of a H-bonding interaction.<sup>9</sup> For the

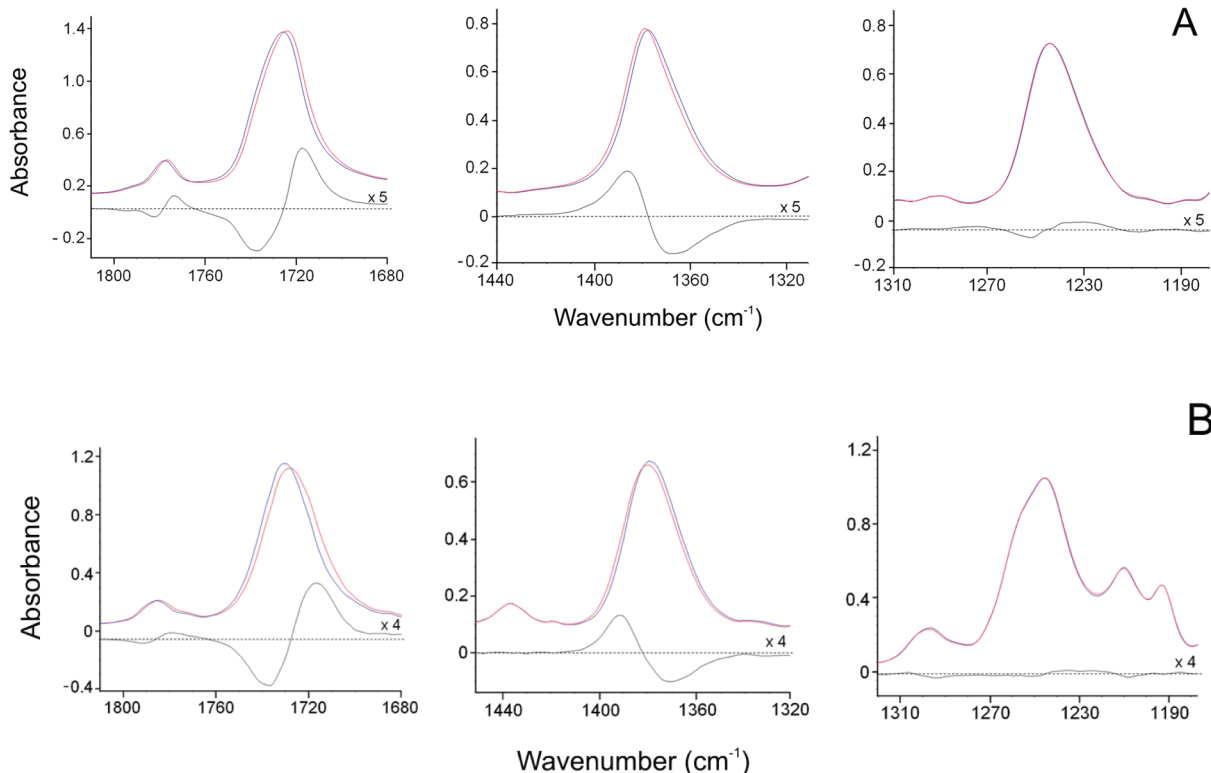


**Figure 11.** Spectra of the dry polyimides (blue traces) of the polyimides equilibrated at  $p/p_0 = 0.6$  (red traces) and difference spectra (wet–dry, black traces). Spectra are reported in three different frequency regions. The difference spectra have been scale-expanded as indicated in the figures to facilitate the comparison. (A) PMDA-ODA polyimide; (B) 6FDA-ODA polyimide.

6FDA-6FpDA, the peak-shifts are barely detectable as a consequence of the very limited amount of sorbed water (data not shown).

The prominent band at 1244 cm<sup>-1</sup> in PMDA-ODA and at 1246 cm<sup>-1</sup> in 6FDA-ODA originates from the ether linkage of the ODA unit (the asymmetric stretching vibration of the C—O—C bond<sup>25,26</sup>). Contrary to what happens to the carbonyl bands, these peaks remain completely unperturbed even at the highest concentrations of sorbed water (no shift in the absorbance spectra and only random noise in the difference spectra are apparent in Figure 11A,B in the 1310–1180 cm<sup>-1</sup> range). Thus, although in principle the ether oxygens could also act as proton acceptors toward water molecules, the spectroscopic evidence allows us to conclude that their involvement in H-bonding, if any, can be safely neglected. The above conclusion is supported by earlier investigations by CP-Mmass NMR spectroscopy, which pointed out that [...] the water molecules aggregate near the imide groups of the imide ring and are most probably bound via hydrogen bonding. Thus, the water protons remain relatively fixed in the polymer matrix at the carbonyl carbon.<sup>27</sup>

Indications in favor of the physical picture we have proposed are also provided by a recent literature report addressing molecular dynamics simulations of water in PMDA-ODA.<sup>28</sup> In fact, in the case of systems containing 1.4% of water (a concentration comparable to those experimentally detected by us), the simulations indicated that, of the total amount of interacting polymer sites, only about 5% are represented by ether groups, the rest being imide carbonyls.

The whole of the spectroscopic results, taken together with previous literature reports on PMDA-ODA,<sup>9</sup> allow us to put forward likely structures for the H-bonding aggregates that are formed in the investigated systems. Thus, the couple water signals

identified in all the three polyimides at 3660–3570 cm<sup>-1</sup>, can be associated, respectively, to the out-of-phase and in-phase stretching modes of H<sub>2</sub>O molecules bound to imide carbonyls via a H-bonding interaction (see structure I in Figure 12). The other two peaks, also identified in all the three polyimides at 3616 and 3470 cm<sup>-1</sup>, can be ascribed to self-associated water in the form of (predominantly) dimers (see structure II below). In particular, the feature at 3616 cm<sup>-1</sup> has been assigned to a  $\nu(O-H)$  localized primarily on the noninteracting O—H bond, whereas the 3470 cm<sup>-1</sup> band was ascribed (predominantly) to the stretching mode of the interacting O—H bond.

The signal identified only in the case of the 6FDA-6pDA at 3700 cm<sup>-1</sup> is to be related to water molecules whose hydrogen atoms are not involved in H-bonding. This species could be an isolated monomer, but such an assignment would not account for the absence of asynchronous correlation with the doublet of the self-associated species. An alternative interpretation considers a water molecule in a self-associated environment that realizes the H-bonding interaction through its oxygen atom as a proton acceptor (see structure III in Figure 12). This species is not spectroscopically distinguishable from a free monomer<sup>29</sup> and is more likely to share the same dynamic behavior with the main self-associated species (for instance, through an instantaneous, concentration independent, interconversion of structures II and III).

As for the implications of the present results in terms of sorption thermodynamics, we explicitly note that the isolated water molecules represented in Figure 12, structure A, coincide with the first layer of penetrant (first hydration layer) in the frame of the multilayer adsorption model of Brunauer, Emmet, and Teller (BET).<sup>30</sup> On the other hand, the water molecules self-associated with their homologues already bound to imide

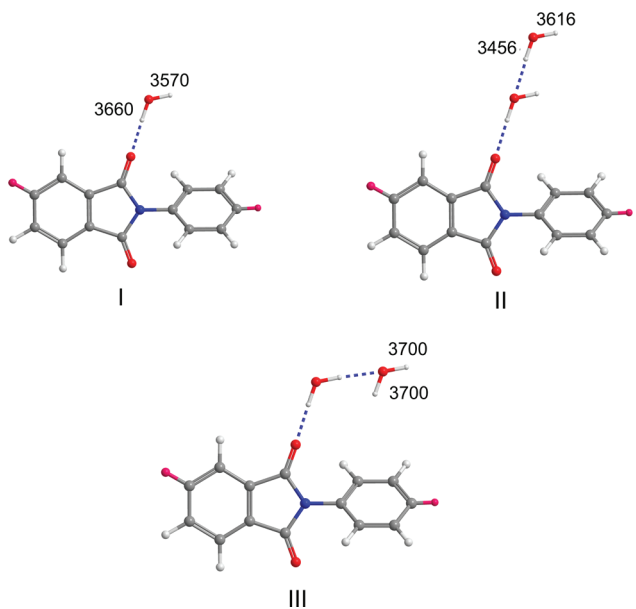


**Figure 12.** Schematic representation of the H-bonding interactions in the investigated water/polyimide systems. Atoms color codes: white = H; gray = C; red = O; blue = N; cyan = dummy. The structures represented are those of the 6FDA-ODA and the 6FDA-6FpDA polyimides. Also indicated are the frequencies of the stretching vibrations of the O–H bonds for the different water species as determined by 2D-COS analysis.

carbyns (Figure 12, structures II and III) are representative of the second-shell hydration layer.

**Quantitative Evaluation of the Water Species.** Toward a quantitative assessment of the concentration of the different water species present in the investigated systems, we first considered the  $\nu_{\text{OH}}$  range (Table 3), owing to its superior resolution.

**Table 3. Results of the Curve-Fitting Analysis in the  $\nu(\text{OH})$  Region for the Three Investigated Polyimides**

	PMDA-ODA	6FDA-ODA	6FDA-6FpDA
position ( $\text{cm}^{-1}$ )			3690
fwhh ( $\text{cm}^{-1}$ )			25
area ( $\text{cm}^{-1}$ )			0.73
position ( $\text{cm}^{-1}$ )	3645	3647	3651
fwhh ( $\text{cm}^{-1}$ )	60	68	68
area ( $\text{cm}^{-1}$ )	16.0	12.4	7.6
position ( $\text{cm}^{-1}$ )	3570	3568	3571
fwhh ( $\text{cm}^{-1}$ )	90	85	84
Area ( $\text{cm}^{-1}$ )	14.4	9.3	10.7
position ( $\text{cm}^{-1}$ )	3470	3495	3492
fwhh ( $\text{cm}^{-1}$ )	180	200	200
area ( $\text{cm}^{-1}$ )	22.2	15.5	6.6

The results of LSCF analysis of the band profile relative to water sorbed at equilibrium into PMDA-ODA at  $p/p_0 = 0.6$  are reported in Figure 13A. We adopted strict criteria to choose the starting model to simulate, upon least-squares minimization, the experimental band profiles. The results of 2D-COS analysis were taken as a guide to establish the number of components and the starting peak positions since 2D spectroscopy substantially improves the resolution in comparison to the conventional frequency spectrum. It is explicitly noted, however, that the number of components detected by 2D-COS

represents a “true” or limiting value, but a peak was included in the curve-fitting model only if it could be discerned in the frequency spectrum by visual inspection and/or second derivative analysis. In summary, the number of components in the LSCF model was lower than or, at most, equal to the number of components detected by 2D-COS.

In particular, according to the 2D-COS results, only a single peak in the  $3500$ – $3300 \text{ cm}^{-1}$  range was used, which gave a very satisfactory simulation of the experimental data-points. In this respect we note that the feature at  $3480 \text{ cm}^{-1}$  does not represent an actual maximum but rather a derivative-type feature appearing in the difference spectrum representative of sorbed water. In fact, this derivative feature occurs as a consequence of the downward shift of the  $3490 \text{ cm}^{-1}$  peak of the polyimide after water sorption. The latter peak is a combination mode of the stretching fundamentals of the imide carbonyls ( $\nu_{\text{ip}} + \nu_{\text{ooph}}$ ), and the shift, as for the respective fundamentals, reflects the occurrence of the H-bonding interaction.<sup>9</sup>

In the case of the 6FDA-6FpDA, the additional component detected at  $3700 \text{ cm}^{-1}$  by 2D-COS is identified by LSCF as a separate contribution located at  $3690 \text{ cm}^{-1}$  (see Figure 13C). It is noted that, for the 6FDA-6FpDA polyimide, the whole  $\nu(\text{OH})$  band-shape changes noticeably with the amount of sorbed water. This is demonstrated in Figure 13D, relative to the spectrum collected at equilibrium for  $p/p_0 = 0.2$ . In this case, the broad component centered at  $3492 \text{ cm}^{-1}$  becomes barely detectable. Recalling the aforementioned spectrum assignments, we may conclude that, for 6FDA-6FpDA, at the lowest values of relative pressure, the monomer interacting with the carbonyl can be considered, to a good approximation, the only species present.

In general, for the three investigated polyimides, owing to the invariance of the water species present, the following relationship can be assumed to hold:

$$\frac{A_{\text{TOT}}}{L} = \sum_{i=1}^N \varepsilon_i C_i \quad (1)$$

where  $A_{\text{TOT}}$  is the total integrated absorbance in the  $\nu_{\text{OH}}$  region,  $A_i$  is the integrated absorbance of the  $i$ th component,  $\varepsilon_i$  is the associated molar absorptivity,  $L$  is the sample thickness, and  $N$  represents the number of individual components in which the experimental profile has been decomposed. If we now choose two analytical peaks characteristic of the species to be quantified, i.e., at  $3568 \text{ cm}^{-1}$  for the monomer and at  $3495 \text{ cm}^{-1}$  for the dimer (the wavenumber values refer to 6FDA-ODA), we may write

$$\frac{A_{3568} + A_{3495}}{L} = \varepsilon_{3568} C_{\text{mon}} + \varepsilon_{3495} C_{\text{dim}} \quad (2)$$

which, taking into account the mass balance

$$C_{\text{TOT}} = C_{\text{mon}} + C_{\text{dim}} \quad (3)$$

can be rearranged as

$$\begin{aligned} \frac{A_{3568} + A_{3495}}{L} &= \varepsilon_{3568} C_{\text{TOT}} + C_{\text{dim}} \\ &\quad (\varepsilon_{3495} - \varepsilon_{3568}) \\ &= \varepsilon_{3568} C_{\text{TOT}} + C_{\text{dim}} \Delta \varepsilon \end{aligned} \quad (4)$$

According to the above equation, if the absorptivity values of the monomer and the dimer were coincident ( $\Delta \varepsilon = 0$ ), a

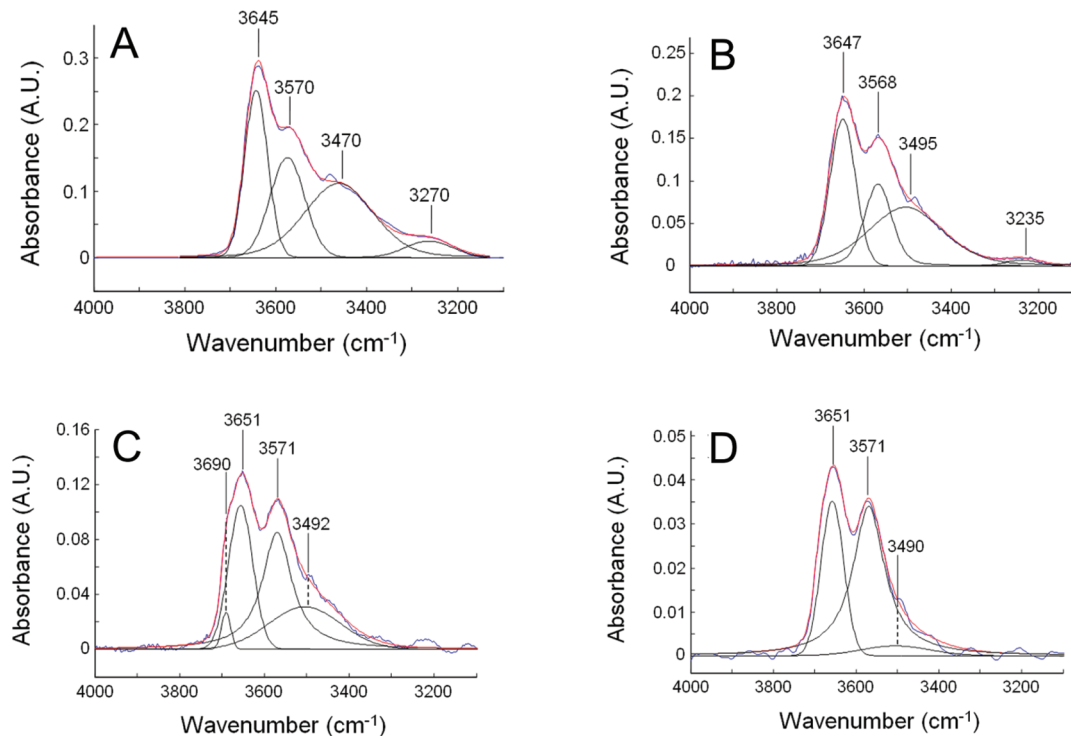


**Figure 13.** LSCF analysis of the  $\nu_{\text{OH}}$  region for (A) PMDA-ODA equilibrated with water vapor at  $p/p_0 = 0.6$ ; (B) 6FDA-ODA equilibrated with water vapor at  $p/p_0 = 0.6$ ; (C) 6FDA-6FpDA equilibrated with water vapor at  $p/p_0 = 0.6$ ; (D) 6FDA-6FpDA equilibrated with water vapor at  $p/p_0 = 0.2$ .

Lambert–Beer diagram would results by plotting  $(A_{3568} + A_{3495})/L$  as a function of  $C_{\text{TOT}}$ . In fact,  $\varepsilon_{\text{dim}}$  exceeds  $\varepsilon_{\text{mon}}$  by an amount proportional to the H-bonding strength; thus the above diagram is expected to display an initial linear trend through the origin in the water concentration range where  $C_{\text{dim}}$  is negligible, i.e., at the lowest values of  $p/p_0$ . Afterward, a significant departure from linearity is expected, which is more pronounced for larger values of  $\varepsilon_{\text{dim}}$  with respect to  $\varepsilon_{\text{mon}}$ , that is, as the H-bonding strength increases. The experimental results, represented in Figure 14, conform to the theoretical predictions.

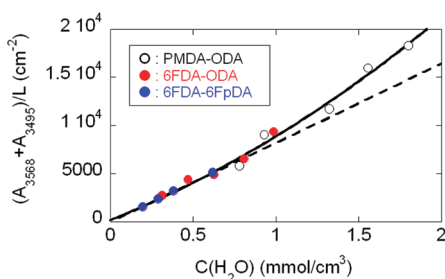


**Figure 14.**  $(A_{3568} + A_{3495})/L$  as a function of water concentration.

The value of  $\varepsilon_{3568}$ , estimated as the tangent at the origin of the best-fitting curve connecting the data of Figure 14, is equal to  $(670 \pm 50) \text{ km mol}^{-1}$ . This absorptivity value allowed us to quantify the concentration of monomeric water in the investigated systems, as well as the concentration of dimers by difference from the total water concentration evaluated gravimetrically (or even spectroscopically from the  $\delta_{\text{HOH}}$  water band, using the calibration curve of Figure 7). To assess the consistency of this method, we plotted the value of  $A_{3495}/L$  as a function of the dimeric water concentration: a linear relationship through the origin resulted (see Figure 15) with a

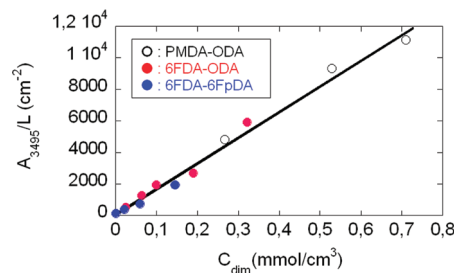


**Figure 15.**  $A_{3495}/L$  as a function of the dimeric water concentration.

slope (corresponding to  $\varepsilon_{3495}$ ) of  $(1700 \pm 100) \text{ km mol}^{-1}$ . A value of  $\varepsilon_{\text{dim}}$  higher than that of  $\varepsilon_{\text{mon}}$  by a factor of 2.5 appears to be consistent, as order of magnitude, with previous results on molar absorptivity increase in similar H-bonding systems.<sup>31</sup>

In Figure 16A–C are reported the concentrations of monomeric water (first-shell layer) and of dimeric water (second-shell layer) as a function of the relative vapor pressure for the three polyimides. In all cases, the majority of the water molecules are located in the first hydration layer, in direct contact with the polymer substrate, although the fraction of water in the second hydration layer increases gradually with the relative pressure of water vapor, i.e., with the total concentration of absorbed water. In particular, for the 6FDA-ODA polyimide, the concentration of water in the first shell seems to reach a plateau at  $p/p_0$  values around 0.6. The distribution of water molecules between the two hydration layers and the related issues will be addressed in a forthcoming paper where the data discussed herein will be interpreted in light of a thermodynamic lattice model accounting for self- and cross-interactions of the H-bonding type.

In Figure 17 is reported the ratio  $C_{\text{First-shell}}/C_{\text{Second-shell}}$  as a function of the total water concentration in the three

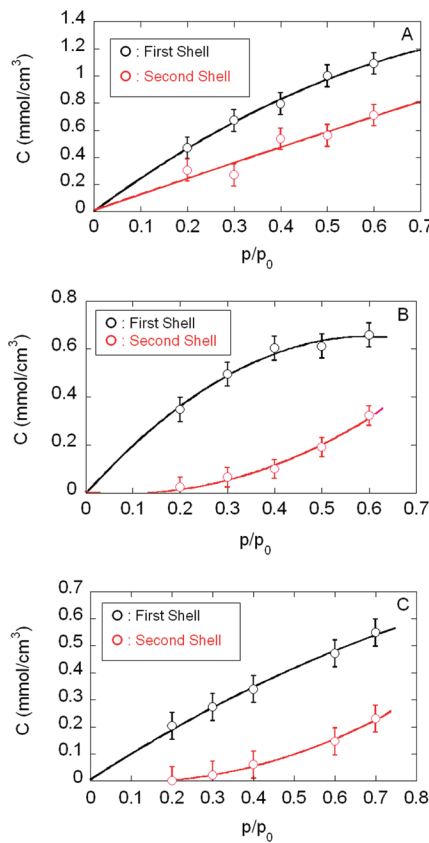


**Figure 16.** Concentration of water present in the first- and second-shell layers as a function of the relative vapor pressure of the sorption test. (A) PMDA-ODA; (B) 6FDA-ODA; (C) 6FDA-6FpDA. Curves connecting the data points are to be intended for eye guidance only.

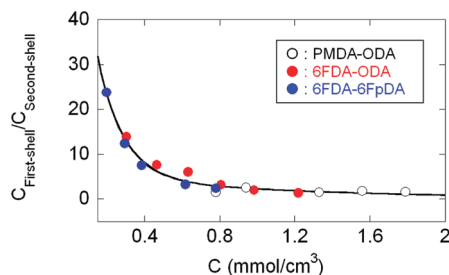


**Figure 17.** The ratio  $C_{\text{First-shell}}/C_{\text{Second-shell}}$  as a function of the total water concentration for the three investigated polyimides.

polyimides. The data exhibit a high level of correlation, but the behavior is specific for each polyimide. In fact, the PMDA-ODA displays almost constant values, while for the 6FDA-6FpDA, the concentration ratio changes by 1 order of magnitude. The 6FDA-ODA, again, shows an intermediate behavior. This effect seems to be related to the amount of water absorbed at equilibrium in the three systems, rather than to the differences in the respective molecular structures.

An alternative approach to quantify the population of water species relies on the shift of the imide carbonyls brought about by the H-bonding interaction. A method of this type has been described in detail in ref 9 and will be summarized hereafter.

It is based on the fact that the observed shift is actually due to the occurrence of two unresolved components originating, respectively, from the interacting carbonyls (at lower frequency) and the unperturbed ones (at higher frequency). The direct

resolution of the components is not achieved owing to their closeness compared to their fwhh. The unperturbed carbonyl peak is experimentally accessible as that of the fully dry polyimide, which can serve as reference for spectral subtraction. Thus, the interacting carbonyl component,  $A_{\text{diff}}$ , can be isolated by subtracting, from the overall experimental profile, the reference peak of the dry polyimide, i.e.,

$$A_{\text{diff}} = A_s - K \cdot A_r \quad (5)$$

where  $A_s$  and  $A_r$  refer, respectively, to the absorbance of the imide peak in the sample spectrum (water saturated film) and the reference spectrum (dry film). Owing to the invariance of the film thickness upon water sorption, the subtraction factor  $K$  contains the information about the relative concentration of the water species. The physical meaning of  $K$ , derived from the relevant absorbance-concentration relationships,<sup>9</sup> is

$$K = \frac{C_f}{C_{\text{TOT}}} \quad \text{and} \quad \frac{C_b}{C_{\text{TOT}}} = 1 - K \quad (6)$$

where the subscripts f, b, and TOT refer, respectively, to the “free” imide groups, the imide groups H-bonded to water molecules, and to their total population. The criterion to correctly choose the subtraction factor  $K$ , is described in ref 9.

By this approach we therefore evaluate the population of interacting proton acceptors (imide carbonyls), while the quantitative analysis in the  $\nu(\text{OH})$  range estimates the concentration of proton donors (water molecules). To directly compare the two values, one must assume a stoichiometry for the water-imide aggregate. In the hypothesis of a 1:1 stoichiometry (see Figure 10, structure I) the concentration of interacting carbonyls is coincident with that of the water molecules in the first hydration layer, so that the quantitative results in the carbonyl and in the  $\nu(\text{OH})$  frequency ranges can be directly compared. Such a comparison is shown in Figure 18A,B for the PMDA-ODA and 6FDA-ODA, respectively. No data are available for the 6FDA-6FpDA polyimide due to the very limited amount of absorbed water, which makes the carbonyl shift barely detectable and unsuitable for quantitative analysis.

The results of the two quantitative approaches compare very satisfactorily for the case of 6FDA-ODA (Figure 18B). The consistency of the data obtained by two fully independent spectroscopic estimates confirms the reliability of the devised methods and adds further support to the proposed structures of the H-bonding molecular aggregates.

For the PMDA-ODA, although the two estimates are comparable in magnitude and exhibit the same trend, the  $\nu(\text{OH})$ -based evaluation is, on average, 30% lower than that resulting from the carbonyl analysis. This discrepancy may have different motivations, among which a less defined stoichiometry of the H-bonding adduct in this specific system appears to be the more likely. In particular, the occurrence of aggregates in which a single water molecule binds two carbonyls (i.e., a 1:2 water/imide stoichiometry) would reduce the overall number of bound water molecules per imide group and move downward the upper curve of Figure 18A to approach its immediately lower counterpart. The estimation of the exact stoichiometry of the water/imide aggregate remains an open issue as it depends on factors like the accessibility of the polymer interactive-site, the molecular architecture of the chain, and the electronic distribution around the proton acceptor. No generalization can therefore be made, but, as a rule of thumb, quantitative methods based on the evaluation of the absolute molar absorptivity of the proton

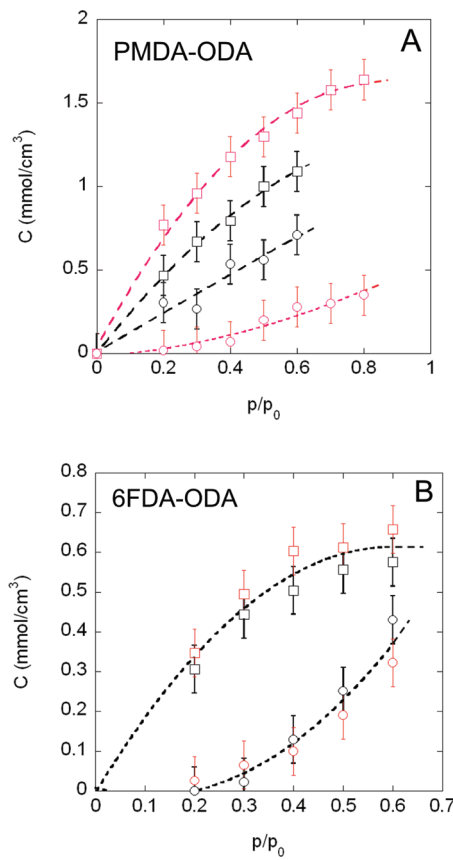


**Figure 18.** Comparison between the concentration of water present in the first-shell layer ( $\square$ ) and in the second-shell layer ( $\circ$ ) as evaluated by analysis of the carbonyl range (red symbols) and the  $\nu(\text{OH})$  range (black symbols). (A) Data relative to the PMDA-ODA polyimide; (B) Data relative to the 6FDA-ODA polyimide.

donor are to be considered more reliable and less stoichiometry-dependent than those based on the intensity ratio of the proton acceptor group.

#### 4. CONCLUDING REMARKS

Gravimetric and time-resolved FTIR measurements of the diffusion process and the sorption equilibrium of water vapor in three polyimides have been carried out with the aim of a molecular level characterization of the mass-transport process and the sorption thermodynamics. Both kinetic and equilibrium measurements have been performed as a function of the relative pressure of water vapor. The spectral data have been analyzed by different and complementary approaches, i.e., difference spectroscopy, least-squares curve fitting, and 2D-COS, which provided the following conclusions: (i) In all the three examined polyimides, two distinct water species were identified, corresponding to single  $\text{H}_2\text{O}$  molecules interacting with the carbonyl groups of the imide functionality, and self-associated water, predominantly dimers. These species can be assumed to correspond to the first- and second-shell hydration layers; (ii) the relative concentration of the two species changes as a function of the total amount of sorbed water; (iii) at the lowest water contents only the monomeric water is present.

A quantitative method has been proposed to quantify the populations of the two water species based on the correlation between gravimetric and spectroscopic data and on the evaluation of the respective molar absorptivities. The results have

been compared with those from an alternative spectroscopic approach previously reported in the literature and based on the analysis of the carbonyl region. Very satisfactory agreement between the two approaches has been obtained for one of the investigated polyimides (6FDA-ODA), while for the PMDA-ODA the carbonyl method consistently overestimated the population of first-shell water. This has been attributed to a less defined stoichiometry of the water/imide aggregate in this specific system.

#### ■ AUTHOR INFORMATION

##### Corresponding Author

\*E-mail: pellegrino.musto@ictp.cnr.it.

#### ■ REFERENCES

- (1) *Polyimides: Fundamentals and Applications*; Gosh, M. K., Mittal, K. L., Eds.; Marcel Dekker: New York, 1996.
- (2) *Advances in Polyimide Science and Technology*; Feger, C., Khojasteh, M. M., Htoo, M. S., Eds.; Technomic: Lancaster, PA, 1993.
- (3) *Polyamic Acids and Polyimides: Synthesis, Transformation and Structure*; Bessonov, M. I., Zubkov, V. A., Eds.; CRC Press: Boca Raton, FL, 1993.
- (4) *Membrane Handbook*; Winston, H. W. S., Sirkar, K. K., Eds.; Kluwer Academic Publishers: Boston, MA, 1992.
- (5) Xiao, Y.; Low, B. T.; Hosseini, S. S.; Chung, T. S.; Paul, D. R. *Prog. Polym. Sci.* **2009**, *34*, 561–580.
- (6) Huang, J.; Cranford, R. J.; Matsuura, T.; Roy, C. *J. Appl. Polym. Sci.* **2003**, *87*, 2306–2317.
- (7) Yang, D. K.; Koros, W. J.; Hopfenberg, H. B.; Stannett, V. T. *J. Appl. Polym. Sci.* **1986**, *31*, 1619–1629.
- (8) Lim, B. S.; Nowick, A. S.; Lee, K. W.; Viehbeck, A. *J. Polym. Sci., Part B: Polym. Phys.* **1993**, *31*, 545–555.
- (9) Musto, P.; Ragosta, G.; Mensitieri, G.; Lavorgna, M. *Macromolecules* **2007**, *40*, 9614–9627.
- (10) Mensitieri, G.; Lavorgna, M.; Larobina, D.; Scherillo, G.; Ragosta, G.; Musto, P. *Macromolecules* **2008**, *41*, 4850–4855.
- (11) Marechal, Y. *J. Mol. Struct.* **2003**, *648*, 27–47.
- (12) Jamroz, D.; Marechal, Y. *J. Mol. Struct.* **2004**, *693*, 35–48.
- (13) Marechal, Y. *J. Mol. Struct.* **1997**, *416*, 133–143.
- (14) Cotugno, S.; Larobina, D.; Mensitieri, G.; Musto, P.; Ragosta, G. *Polymer* **2001**, *42*, 6431–6438.
- (15) Cotugno, S.; Mensitieri, G.; Musto, P.; Sanguigno, L. *Macromolecules* **2005**, *38*, 801–811.
- (16) Ragosta, G.; Musto, P.; Abbate, M.; Scarinzi, G. *J. Appl. Polym. Sci.* **2011**, *121*, 2168–2186.
- (17) Mensitieri, G.; Cotugno, S.; Musto, P.; Ragosta, G.; Nicolais, L. Transport of Water in High  $T_g$  Polymers: A Comparison Between Interacting and Non-interacting Systems. In *Polyimides and Other High Temperature Polymers: Synthesis, Characterization and Applications*; Mittal, K.L., Ed.; VSP Publishing: The Netherlands, 2003, Vol. 2, pp 267–285.
- (18) Marquardt, D. W. *J. Soc. Ind. Appl. Math.* **1963**, *11*, 431–441.
- (19) Meier, R. J. *Vib. Spectrosc.* **2005**, *39*, 266–269.
- (20) Berens, A. R. *Die Angew. Makromol. Chem.* **1975**, *47* (1), 97–110.
- (21) Zimm, B. H.; Lundberg, L. *J. Phys. Chem.* **1956**, *60* (4), 425–428.
- (22) *Handbook of Vibrational Spectroscopy*; Chalmers, J. M., Griffiths, P. R., Eds.; Wiley: Chichester, U.K., 2002; Vol. 3, pp 2225–2234.
- (23) Noda, I.; Ozaki, Y. *Two-Dimensional Correlation Spectroscopy*; Wiley: Chichester, U.K., 2004.
- (24) Noda, I.; Dowrey, A. E.; Marcott, C.; Story, G. M.; Ozaki, Y. *Appl. Spectrosc.* **2000**, *54*, 236A–248A.
- (25) Ishida, H.; Wellinghoff, S. T.; Baer, E.; Koenig, J. L. *Macromolecules* **1980**, *13*, 826–834.
- (26) Saini, A. K.; Carlin, C. M.; Patterson, H. H. *J. Polym. Sci., A* **1992**, *30*, 419–427.

- (27) Waters, J. F.; Likavec, W. R.; Ritchey, W. M. *J. Appl. Polym. Sci.* **1994**, *53*, 59–70.
- (28) Marque, G.; Neyertz, S.; Verdu, J.; Prunier, V.; Brown, D. *Macromolecules* **2008**, *41*, 3349–3362.
- (29) Choppin, G. R.; Violante, M. R. *J. Chem. Phys.* **1972**, *56*, 5890–5898.
- (30) Brunauer, S.; Emmett, P. H.; Teller, E. *J. Am. Chem. Soc.* **1938**, *60*, 309–319.
- (31) Pimentel, G. C.; McClellan, L. *The Hydrogen Bond*; Freeman and Co.: San Francisco, CA, 1960.